

Nystatin Drug as an Effective Corrosion Inhibitor for Mild Steel in Acidic Media– An Experimental and Theoretical Study

Valbonë Mehmeti[†]

University of Prishtina, Faculty of Agriculture and Veterinary, Prishtina, Kosovo
(Received September 04, 2021; Revised October 13, 2021; Accepted October 13, 2021)

Potentiodynamic polarization, EIS measurements, quantum chemical calculations, and molecular dynamic simulations were used to investigate the corrosion behavior of mild steel in 0.5 M aqueous hydrochloric acid medium in the presence or absence of nystatin drug. Potentiodynamic tests suggested that this molecule could act as a mixed inhibitor due to its adsorption on the mild steel surface. The objective of this study was to exploit theoretical calculations to gain a better understanding mechanism of inhibition. Calculating the adsorption behavior of the investigated molecule on Fe (1 1 0) surface was accomplished using Monte Carlo simulation. Molecules were also investigated using Density Functional Theory (DFT), specifically PBE functional, in order to identify the link between molecular structure and corrosion inhibition behavior of the compound under investigation. Adsorption energies between nystatin and iron were estimated more accurately by utilizing Molecular Mechanics calculation with Periodic Boundary Conditions (PBC). Estimated theoretical parameters significantly assisted our understanding of the corrosion inhibition mechanism exhibited by this molecule. They were found to be in accord with experimental results.

Keywords: Corrosion inhibition, Nystatin, Tafel plots, DFT, MC and MD

1. Introduction

A combination of the physical and chemical characteristics of mild steel, as well as its low availability and cost, have made it one of the most widely used materials in a wide range of industrial areas [1–6]. This material is utilized in a variety of applications, including mineral processing equipment, petroleum refining, and other construction applications. Despite the fact that the material has a wide range of applications, it has poor corrosion resistance when exposed to aqueous solutions of hydrochloric acid. As a result of this exposure, many metal structures deteriorate, resulting in significant economic repercussions. As a result, corrosion protection has become an inevitability. Several techniques have been tried to safeguard metals, but one of the most successful and cost-effective is the addition of inhibitors to an acid media. According to the literature, organic compounds that include unsaturated bonds, aromatic rings as well as heteroatoms such as O, N, and S, are the most effective corrosion inhibitors [7–10]. Using mild steel in 0.5 M

HCl, we investigated the inhibitory impact of nystatin drug on the corrosion of this material. Nystatin is a possible corrosion inhibitor due to its chemical structure, which contains heteroatoms (O, N) and numerous double bonds. Theoretical calculations (DFT, MC and MD) were used to complete the study.

2. Materials and Methods

2.1 Instrument, material, electrode preparation and the corrosive solution

At 298 K, a PalmSens3 potentiostat was utilized in conjunction with a three-electrode cell. As an auxiliary electrode, a graphite rod ($d = 3$ cm, $l = 4$ cm) was used, and the saturated calomel electrode (SCE) was used as a reference electrode. Potentiodynamic polarization curves were produced by scanning the electrode potential vs. E_{OCP} at a 1 mV/s sweep rate. The measurements were performed in an atmospheric environment. Each experiment was accomplished three times to ensure repeatability. The EIS measurements were performed at the frequency range from 5 Hz to 10000 Hz at the Open Circuit Potential (OCP) and using an amplitude perturbation

[†]Corresponding author: valbona.mehmeti@uni-pr.edu

Table 1. Composition of mild steel (wt%)

Fe	C	P	Mn	Si	Cr	S	Mo	Ni
99.54	0.1252	0.0316	0.1836	0.0561	0.0124	0.0282	0.0125	0.0015

of 10 mV.

Table 1 shows the mass percentages of mild steel (in weight percent) [11]. The corrosive solution utilized was a 0.5 M HCl acid solution that was prepared by diluting the solution with bi-distilled water.

The electrode for the electrochemical experiments was made by embedding a mild steel rod ($d = 1.5$ mm, $l = 15$ mm) within a Teflon[®] tube ($d = 0.5$ cm, $l = 5$ cm) with epoxy glue and then allowing the electrode to dry. The electrode was polished on silicon carbide abrasive paper (medium grain diameter 6.5–15.3 microns), then on a (DP-Nap) cloth soaked in aluminum oxide (0.3 micron particle size) solution, and then washed and sonicated in water.

2.2 DFT calculations

DFT calculations were fulfilled by the Dmol³ software from Biovia [12,13]. Meta Generalized Gradient Approximation [14,15] employing the M11-L [15-17] and the Double Numeric quality basis set (DNP) [18] were used for geometry optimizations (using the Grimme's DFT-D correction). A lower than 0.00001 kcal/mol convergence standard for the self-consistent-field (SCF) was used for the SCF. The energy minima were validated by carrying out a vibrational analysis and establishing that there were no imaginary frequencies present in the data [19-21].

2.3 Monte Carlo (MC) and Molecular Dynamic (MD) simulation

The simulation of the interaction of a mild steel surface with the Nystatin drug is performed in the corrosion environment by utilizing a six atom-thick layer unit cell of Fe(1 1 0) surface as the basis for the experiment (under Periodic Boundary Condition). The surface of Fe(110) is densely packed; it has a lower surface energy but a higher surface atom coordination number. As a result, this surface was chosen to address the adsorption of Nystatin largely because it has a greater number of interaction sites with corrosion inhibitor. The sizes of the slab model were: $32.271 \text{ \AA} \times 32.271 \text{ \AA} \times 10.235 \text{ \AA}$ with and enclosed

addition of a 30 Å vacuum layer at the C axis that was introduced with: 1 Nystatin molecule / 1000 H₂O molecules / 10 chloride + 10 hydronium ions. In advance of the MD step, the geometry of the simulation boxes was optimized (energy converges tolerance of: 1×10^{-5} kcal/mol) using the Forcite module in the Biovia software package.

MD was performed at a temperature of 25 °C [22] using the Constant volume/constant temperature (NVT) canonical ensemble with a simulation period of 1000 ps [23-27]. The Berendsen thermostat conserves the temperature. Calculations for MC and MD are carried out using the Condensed Phase Optimized Molecular Potential II (COMPASSII) forcefield. [26,28-37]. Radial Distribution Function (RDF) analysis included the entire MD trajectory [2,20,23,29].

3. Results and Discussion

3.1 Polarization measurements

The anodic and cathodic polarization curves of a mild steel electrode in 0.5 M HCl solution are shown in Fig. 1 in the absence and presence of the drug Nystatin at 298 K. The IE (in percent) was determined using equation (1):

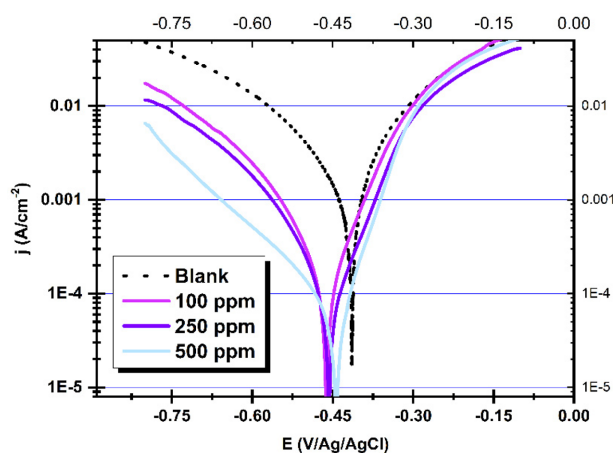


Fig. 1. The Tafel plot of the mild steel electrode measured in HCl solution ($c = 0.5$ M): in the absence and in the presence of: 100, 200 and 500 ppm of Nystatin

Table 2. Electrochemical parameters of mild steel at various concentrations of Nystatin molecule in 0.5 M HCl

C [ppm]	E_{corr} [V]	I_{corr} [$\mu\text{A}/\text{cm}^2$]	bc [mV/dec]	Bc [mV/dec]	IE [%]
-	-0.419	803.7	-143.1	89.4	-
100	-0.463	149.2	-108.3	74.5	81.43
250	-0.451	99.4	-110.1	56.4	87.63
500	-0.442	52.3	-116.8	54.1	93.49

$$IE(\%) = \frac{i_{corr, absence\ of\ inhibitor} - i_{corr, presence\ of\ inhibitor}}{i_{corr, absence\ of\ inhibitor}} \times 100 \quad (1)$$

The electrochemical parameters: corrosion potential (E_{corr}) and corrosion current density (i_{corr}), were determined from the intersection of anodic and cathodic Tafel slopes and are presented in Table 2.

The Tafel plot in Fig. 1 demonstrates that adsorption of Nystatin molecules onto the mild steel surface substantially lowers the corrosion current of the mild steel in this hostile environment, reflecting a high corrosion inhibition effectiveness of up to 93.49 percent.

When Nystatin is added to the solution, the values of the cathodic and anodic Tafel slopes (bc, ba) (Table 1) alter. The variations in the Tafel slopes indicate that both molecules have an effect on the kinetics of the hydrogen evolution process [10]. This results in a greater energy barrier for proton discharge and therefore less gas evolution. The investigated compound had no discernible effect on the corrosion potential, suggesting that it acts as a mixed-type inhibitor [6].

3.2 EIS measurements

The different electrochemical parameters derived from these spectra using the electrical circuit of Fig. 2 are given in Table 3.

As illustrated in Fig. 3, impedance diagram is defined

by a single capacitive loop centered on the real axis, the diameter of which grows as the inhibitor concentration increases, suggesting an increase in protective power. This

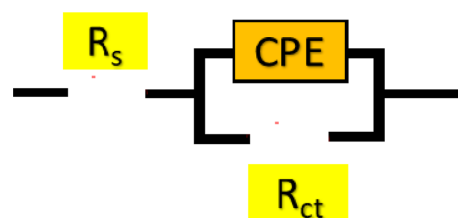


Fig. 2. Equivalent circuit for fitting the experimental impedance data

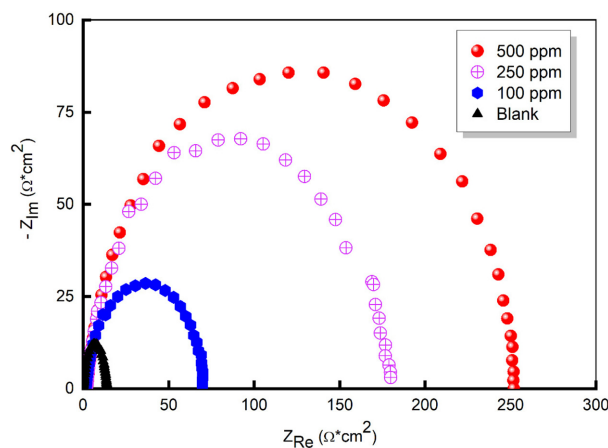


Fig. 3. Nyquist plots of the mild steel electrode measured in HCl solution (c = 0.5 M): in the absence and in the presence of: 100, 200 and 500 ppm of Nystatin

Table 3. EIS and the corresponding inhibition efficiencies for mild steel in 0.5 M HCl solution in the absence and presence of various concentrations Nystatin at 298 K

	Conc. (ppm)	R_s ($\Omega\ \text{cm}^2$)	R_{ct} ($\Omega\ \text{cm}^2$)	n_{dl}	C_{dl} ($\mu\text{F}\cdot\text{cm}^2$)	Q ($\mu\text{F}\cdot\text{S}^{n-1}$)	θ	η_{imp} %
HCl 0.5 M	--	2.07	10.2	0.89	187.2	530.1	-	-
Nystatin	500	1.58	251.1	0.75	55.4	134.3	0.959	95.9
	250	1.67	169.4	0.79	74.7	178.9	0.939	93.9
	100	2.04	66.3	0.81	89.2	206.4	0.846	84.6

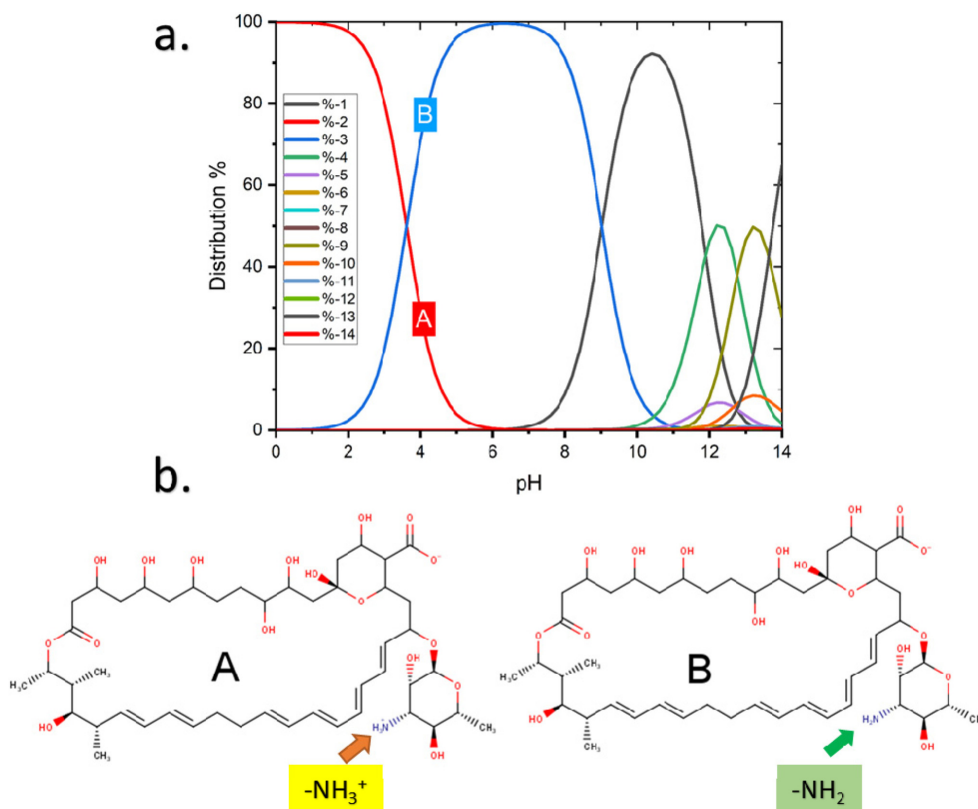


Fig. 4. a. the distribution percentage of Nystatin molecular forms vs. pH value of the media and b. two major species distributed at $\text{pH} < 7$ used in the theoretical calculations (DFT, MC and MD)

finding reveals that the load transfer process is the primary determinant of the corrosion reaction of mild steel with and without protection [38]. Additionally, the Nyquist plots are not ideal half-loops, which may be a result of the interfacial impedance frequency dispersion due to the roughness and heterogeneity of the metal surface [31].

As shown in Table 3, as the concentration of Nystatin increases, the charge transfer resistance increases and the Q declines from 500 to 150 ppm, which can be attributed to the reinforcement of the test film adsorbed on the steel surface.

3.3 DFT, MC and MD results

Prior to calculation, the microspecies distribution of the Nystatin molecule was calculated using Chemaxon software to account for pH impact on protonation/deprotonation. As seen in Fig. 4a. Forms A and B of the chemical structures are both below pH 7 and these structures were used in the theoretical calculations (Fig. 4b).

When it comes to molecular simulation and mechanism verification, both HOMO and LUMO (Fig. 5) are often

used as guidelines to give information on whether a reaction is proceeding correctly and which portions of the molecules are accountable for the reaction [6,30,31]. While the HOMO shows electrons being donated to the electron-accepting portions of the molecule, the LUMO depicts electrons being donated to the net-donor sections of the molecule.

On the other hand, the HOMO and LUMO OM and MEP of the Nystatin drug are shown in Fig. 5, and the most often seen DFT indices are listed in Table 4. Most of the HOMO and LUMO densities are concentrated around the sugar moiety in the part of the molecule holding the double bonds. When it comes to the Nystatin, the noteworthy importance of HOMO and LUMO is their capacity to interact with the Fe(1 1 0) surface via electron donation and acceptance, respectively [2,7,37-40,24-27,29-32].

This trend is also evident when the electron affinity and ionization potential of the material are calculated, resulting in a similar capacity. Additionally, an acceptable softness value and a somewhat low hardness ratio enhance

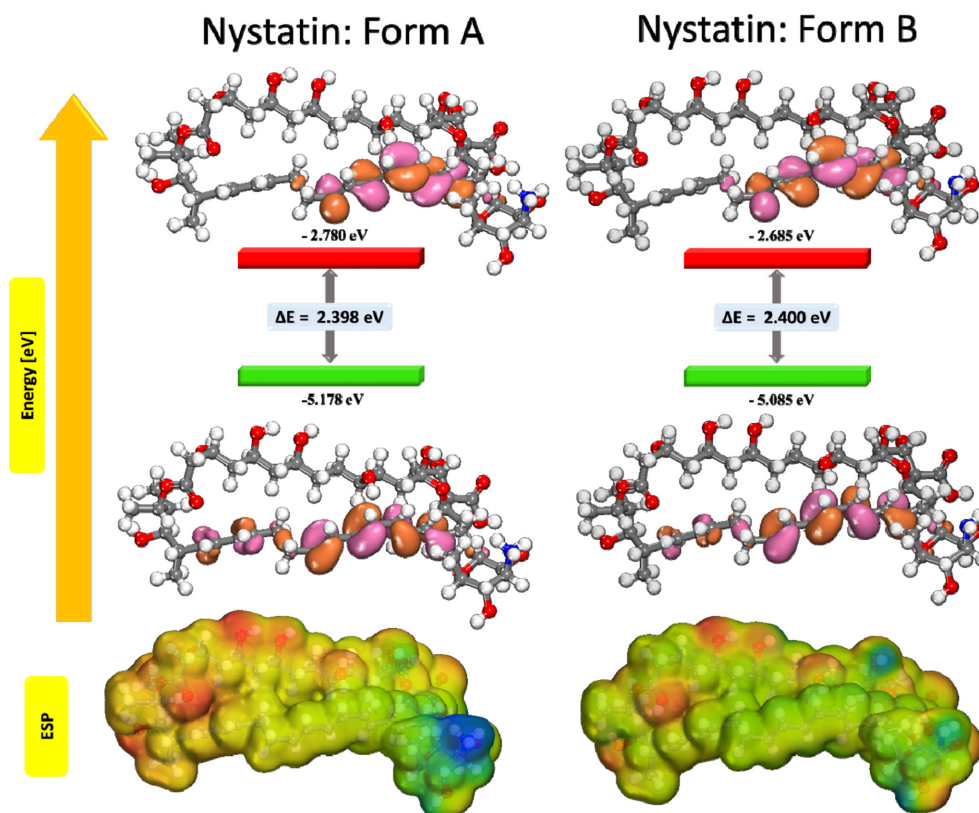


Fig. 5. HOMO, LUMO surfaces and ESP for Nystatin molecule

Table 4. Calculated theoretical chemical parameters for the Nystatin inhibitor.

Theoretical parameters	Nystatin Form A	Nystatin Form B
HOMO	-5.178	-5.085
LUMO	-2.780	-2.685
ΔE (HOMO-LUMO)	2.398	2.400
Ionization energy (I)	5.178	5.085
Electron affinity (A)	2.780	2.685
Electronegativity (X)	3.979	3.885
Global hardness (η)	1.199	1.200
Chemical potential (π)	-3.979	-3.885
Global softness (σ)	0.834	0.833
Global electrophilicity (ω)	6.602	6.289
Electrodonating (ω^-) power	8.742	8.381
Electroaccepting (ω^+) power	4.763	4.496
Net electrophilicity ($\Delta\omega^+$)	4.648	4.377
Fraction of transferred electrons (ΔN)	-0.312	-0.273
Energy from Inhb to Metals (ΔN)	0.117	0.089
ΔE back-donation	-0.300	-0.300

Nystatin's propensity for adsorption on metal surfaces [9,11,41,42].

3.4 Monte Carlo and Molecular dynamic simulations

The lowest energy configurations of the Nystatin molecule on the metal surface in the simulated corrosion environment are shown in Fig. 6. The adsorption geometries of the inhibitor indicate that the oxygen atoms help in the adsorption process. This adsorption affinity results in the development of a protective anti-corrosion layer on the metal surface.

The quantitative determination of the inhibitor molecule's interaction with the metal surface is accomplished via the computation of the adsorption energies using the following equation [43]:

$$E_{ads} = E_{total} - [E_{surface + water} + E_{Nystatin}] + E_{water}$$

where: E_{total} is the total energy of the system as a result of inhibitor-metal interaction; $E_{surface + water}$ and $E_{Nystatin + water}$ is system energy in the absence and presence of Nystatin inhibitor.

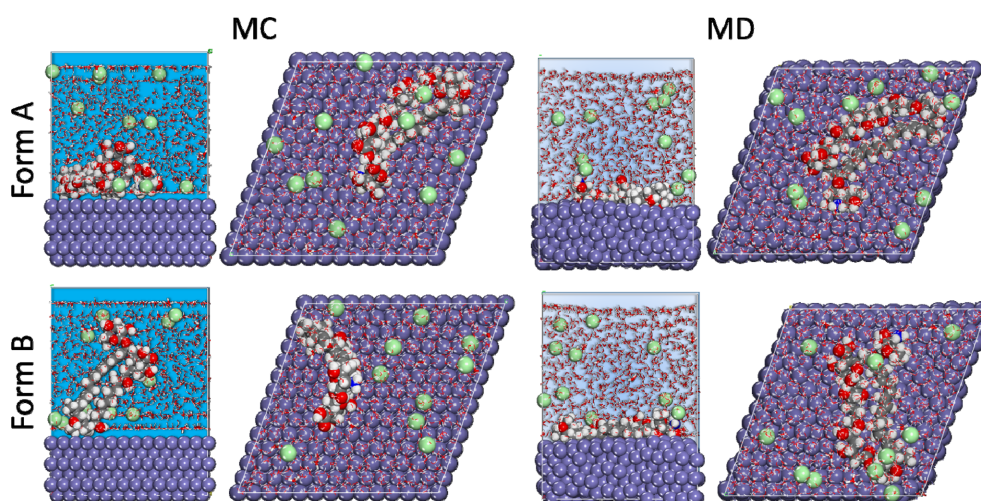


Fig. 6. A. MC and B. MD obtained from the adsorption configurations of the Nystatin inhibitor in the simulated corrosion media on the Fe surface

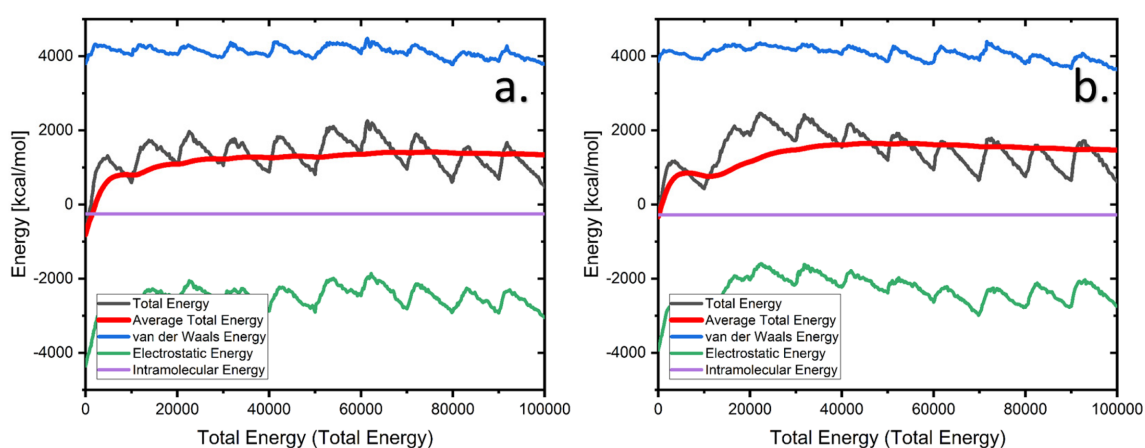


Fig. 7. The contribution of the different energy terms during the MC calculations (a. Form a and b. Form b)

Random molecular configurations as big as feasible (ions or molecules) are selected in the simulation box for each MC. The graph in Fig. 7 shows that as more of these systems are utilized, the average energy of the system reaches a plateau, indicating that the system has achieved its energy equilibrium (after 45000 steps).

The identical number of randomly generated MC configurations (one million) was utilized for both Nystatin forms, and the lowest energy configurations as indicated by the stability of the Average Total Energy values were obtained. The different energy terms are the results of the functional form of the COMPASS II force field (consisting of terms for: bonds, angles, dihedrals, out-of-plane angles as well as cross-terms, and two non-bonded functions, a Coulombic function for electrostatic interactions

and a Lennard-Jones potential for van der Waals interactions). The deprotonation of the amino group appears to have a little effect on the Nystatin molecule's interaction with the mild steel surface.

Monte Carlo simulations agree well with the experimental findings. The high negative value of the adsorption energies (Fig. 8) attests to the adsorption process's spontaneity [11,24,25,34].

MD simulations retain the ability to track and record the dynamics of the adsorption of the inhibitor on the metal surface [31,44-47]. One method to verify that the system achieved the lowest energy, it is to monitor the potential temperature change throughout the MD run. From the Fig. 9, the temperature drift is low – indicating a successful run of the MD of our system.

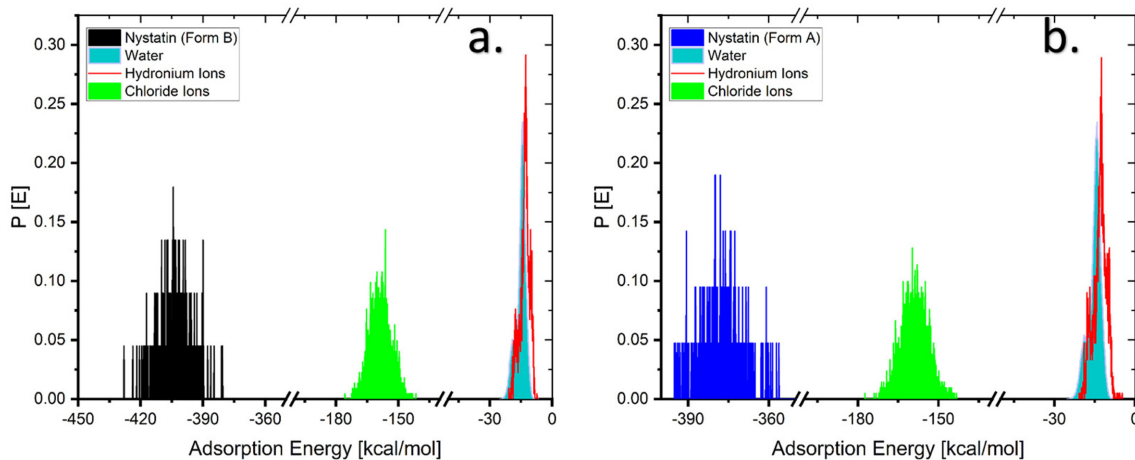


Fig. 8. Distribution of the adsorption energies for Nystatin (a. Form a and b. Form b) onto the iron surface obtained by via MC

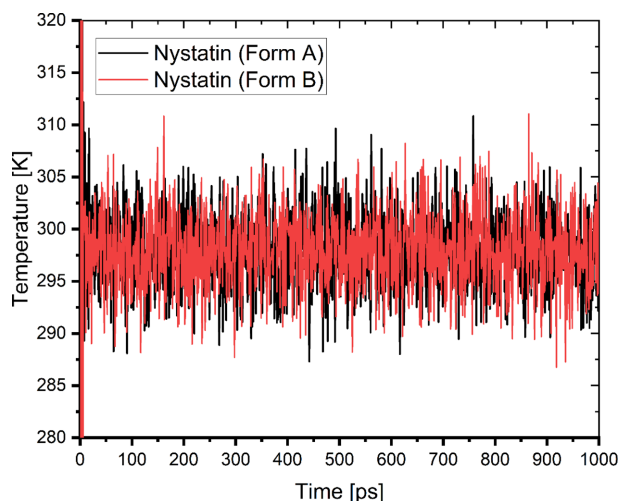


Fig. 9. Temperature fluctuation ($T = 298$ K) during the MD run in the simulated corrosion media

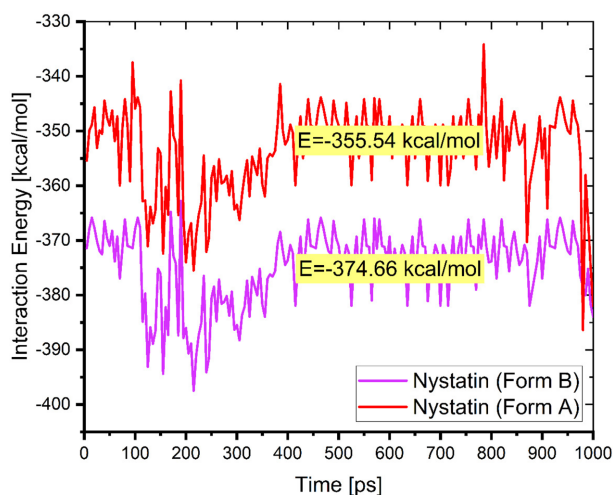


Fig. 10. Evolution of the adsorption energy during the MD run in the simulated corrosion media during the interaction of Nystatin (Form A and B) with Fe (1 1 0) surface in the simulated corrosion media (the corresponding mean values of the interaction energies are presented in the graph)

The latest inhibitor configurations on the metal surface are shown in Fig. 6. The MC calculations indicate that the O atoms are responsible for the Nystatin drug's adsorption. The adsorption energy derived from the MD simulations (Fig. 10) demonstrates that since the inhibitor regardless of its protonation form (A or B) interacts strongly with the surface, it lays nearly flat on it, limiting the ability of corrosion species to reach the surface – thus reducing the mild steel's corrosion rate.

This deduction is sustained also by the analysis of the Radial Distribution Function (RDF) calculated the oxygen atoms from the horizontal of the metal surface presented in the Fig. 11.

It is widely accepted that when a peak appears in the

RDF graph of a particular atom(s) and the surface between 1 and 3.5 Å, it is a strong indication that chemisorption occurred, whereas the presence of physisorption RDF peaks is estimated at greater distances (typically > 3.5 Å) [22,23,25,32-35,39].

The RDF for the oxygen atoms (Fig. 9) of the inhibitor suggests the chemisorption of the inhibitor on the metal surface [48,49]. The accomplished results from MD and corresponding RDF analysis validate the firm tendency of the inhibitors to adsorb and protect the metal, due to its unusual attraction to bring and take electrons to the metal surface [23,38,41].

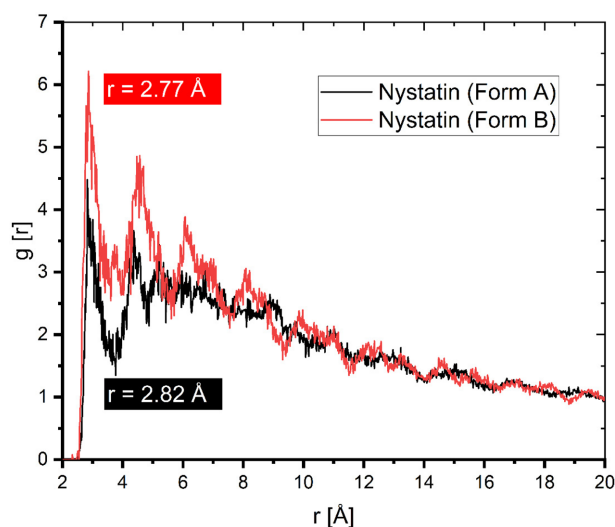


Fig. 11. RDF oxygen and nitrogen atoms for the Nystatin inhibitor onto Fe(1 1 0) surface gained via MD

4. Conclusions

The studied molecule is an excellent inhibitor for mild steel in an acidic medium. The polarization measurements show that this molecule acts as a mixed inhibitor. DFT calculations were used to determine the inhibitors' adsorption centers. Additionally, the MC and MD calculations support the inhibitor's strong adsorption interaction with the metal surface, providing molecular evidence for the Nystatin molecule's adsorption behavior (geometry) and adsorption energy on the iron surface. Theoretical results (DFT, MC, and MD) corroborate the experimental results.

References

1. N. Yilmaz, A. Fitoz, Ü. Ergun, K. C. Emregül, A combined electrochemical and theoretical study into the effect of 2-((thiazole-2-ylimino)methyl)phenol as a corrosion inhibitor for mild steel in a highly acidic environment, *Corrosion Science*, **111**, 110 (2016). Doi: <https://doi.org/10.1016/j.corsci.2016.05.002>
2. M. Rbaa, M. Ouakki, M. Galai, A. Berisha, B. Lakhrissi, C. Jama, I. Warad, A. Zarrouk, Simple preparation and characterization of novel 8-Hydroxyquinoline derivatives as effective acid corrosion inhibitor for mild steel: Experimental and theoretical studies, *Colloids Surfaces A Physicochemical and Engineering Aspects*, **602**, 125094 (2020). Doi: <https://doi.org/10.1016/j.colsurfa.2020.125094>
3. H. Lgaz, R. Salghi, A. Chaouiki, Shubhalaxmi, S. Jodeh, K. Subrahmanya Bhat, Pyrazoline derivatives as possible corrosion inhibitors for mild steel in acidic media: A combined experimental and theoretical approach, *Cogent Eng.*, **5** (2018). Doi: <https://doi.org/10.1080/23311916.2018.1441585>
4. N. A. Odewunmi, M. A. Jafar Mazumder, S. A. Ali, N. A. Aljeaban, B. G. Alharbi, A. A. Al-Saadi, I. B. Obot, Impact of Degree of Hydrophilicity of Pyridinium Bromide Derivatives on HCl Pickling of X-60 Mild Steel: *Experimental and Theoretical Evaluations, Coatings*, **10**, 185 (2020). Doi: <https://doi.org/10.3390/coatings10020185>
5. A. Al-Amiery, A. Kadhum, A. H. Alobaidy, A. Mohamad, P. Hoon, Novel Corrosion Inhibitor for Mild Steel in HCl, *Materials*, **7**, 662 (2014). Doi: <https://doi.org/10.3390/ma7020662>
6. A. Berisha, F. Podvorica, V. Mehmeti, F. Sylja, D. Vataj, Theoretical and experimental studies of the corrosion behavior of some thiazole derivatives toward mild steel in sulfuric acid media, *Macedonian Journal of Chemistry and Chemical Engineering*, **34**, 287 (2015). Doi: <http://dx.doi.org/10.20450/mjccce.2015.576>
7. R. Hsissou, O. Dagdag, S. About, F. Benhiba, M. Berardi, M. El Bouchti, A. Berisha, N. Hajjaji, A. Elharfi, Novel derivative epoxy resin TGETET as a corrosion inhibition of E24 carbon steel in 1.0 M HCl solution. Experimental and computational (DFT and MD simulations) methods, *Journal of Molecular Liquids*, **284**, 182 (2019). Doi: <https://doi.org/10.1016/j.molliq.2019.03.180>
8. R. Hsissou, F. Benhiba, S. Echihi, S. Benkhaya, M. Hilali, A. Berisha, S. Briche, A. Zarrouk, K. Nouneh, A. Elharfi, New epoxy composite polymers as a potential anticorrosive coatings for carbon steel in 3.5% NaCl solution: Experimental and computational approaches, *Chemical Data Collections*, **31**, 100619 (2021). Doi: <https://doi.org/10.1016/j.cdc.2020.100619>
9. M. Rbaa, P. Dohare, A. Berisha, O. Dagdag, L. Lakhrissi, M. Galai, B. Lakhrissi, M. E. Touhami, I. Warad, A. Zarrouk, New Epoxy sugar based glucose derivatives as eco friendly corrosion inhibitors for the carbon steel in 1.0 M HCl: Experimental and theoretical investigations, *Journal of Alloys and Compounds*, **833**, 154949 (2020) Doi: <https://doi.org/10.1016/j.jallcom.2020.154949>
10. A. Molhi, R. Hsissou, M. Damej, A. Berisha, V. Thaçi, A. Belafhaili, M. Benmessaoud, N. Labjar, S. El Hajjaji, Contribution to the corrosion inhibition of C38 steel in 1 M hydrochloric acid medium by a new epoxy resin

- PGEPPP, *The International Journal of Corrosion and Scale Inhibition*, **10**, 399 (2021). Doi: <http://dx.doi.org/10.17675/2305-6894-2021-10-1-23>
11. V. V. Mehmeti, A. R. Berisha, Corrosion study of mild steel in aqueous sulfuric acid solution using 4-methyl-4h-1,2,4-triazole-3-thiol and 2-mercaptonicotinic acid-an experimental and theoretical study, *Frontiers in Chemistry*, **5**, 61 (2017). Doi: <https://doi.org/10.3389/FCHEM.2017.00061>
 12. B. Delley, From molecules to solids with the DMol3 approach, *The Journal of Chemical Physics*, **113**, 7756 (2000). Doi: <https://doi.org/10.1063/1.1316015>
 13. J. Andzelm, R. D. King-Smith, G. Fitzgerald, Geometry optimization of solids using delocalized internal coordinates, *Chemical Physics Letters*, **335**, 321 (2001). Doi: [https://doi.org/10.1016/S0009-2614\(01\)00030-6](https://doi.org/10.1016/S0009-2614(01)00030-6)
 14. J. P. Perdew, K. Burke, M. Ernzerhof, Generalized gradient approximation made simple, *Physical Review Letters*, **77**, 3865 (1996). Doi: <https://doi.org/10.1103/PhysRevLett.77.3865>
 15. A. Berisha, Interactions between the aryl diazonium cations and graphene oxide: A DFT study, *Journal of Chemistry*, **2019**, Article ID 5126071 (2019). Doi: <https://doi.org/10.1155/2019/5126071>
 16. J. P. Perdew, K. Burke, M. Ernzerhof, Perdew, Burke, and Ernzerhof Reply, *Physical Review Letters*, **80**, 891 (1998). <https://doi.org/10.1103/PhysRevLett.80.891>
 17. N. Mardirossian, M. Head-Gordon, Thirty years of density functional theory in computational chemistry: An overview and extensive assessment of 200 density functionals, *Molecular Physics*, **115**, 2315 (2017). Doi: <https://doi.org/10.1080/00268976.2017.1333644>
 18. Y. Inada, H. Orita, Efficiency of numerical basis sets for predicting the binding energies of hydrogen bonded complexes: Evidence of small basis set superposition error compared to Gaussian basis sets, *Journal of Computational Chemistry*, **29**, 225 (2008). Doi: <https://doi.org/10.1002/jcc.20782>
 19. B. Delley, Ground-state enthalpies: Evaluation of electronic structure approaches with emphasis on the density functional method, *The Journal of Physical Chemistry A*, **110**, 13632 (2006). Doi: <https://doi.org/10.1021/jp0653611>
 20. A. Alija, D. Gashi, R. Plakaj, A. Omaj, V. Thaçi, A. Reka, S. Avdiaj, A. Berisha, A theoretical and experimental study of the adsorptive removal of hexavalent chromium ions using graphene oxide as an adsorbent, *Open Chemistry*, **18**, 936 (2020). Doi: <https://doi.org/10.1515/chem-2020-0148>
 21. A. Berisha, First principles details into the grafting of aryl radicals onto the free-standing and borophene/Ag(1 1 1) surfaces, *Chemical Physics*, **544**, 111124 (2021). Doi: <https://doi.org/10.1016/j.chemphys.2021.111124>
 22. V. Thaçi, R. Hoti, A. Berisha, J. Bogdanov, Corrosion study of copper in aqueous sulfuric acid solution in the presence of (2E,5E)-2,5-dibenzylidenecyclopentanone and (2E,5E)-bis[(4-dimethylamino)benzylidene]cyclopentanone: Experimental and theoretical study, *Open Chemistry*, **18**, 1412 (2020). Doi: <https://doi.org/10.1515/chem-2020-0172>
 23. R. Hsissou, F. Benhiba, S. About, O. Dagdag, S. Benkhaya, A. Berisha, H. Erramli, A. Elharfi, Trifunctional epoxy polymer as corrosion inhibition material for carbon steel in 1.0 M HCl: MD simulations, DFT and complexation computations, *Inorganic Chemistry Communications*, **115**, 107858 (2020). Doi: <https://doi.org/10.1016/j.inoche.2020.107858>
 24. R. Hsissou, S. About, R. Seghiri, M. Rehioui, A. Berisha, H. Erramli, M. Assouag, A. Elharfi, Evaluation of corrosion inhibition performance of phosphorus polymer for carbon steel in [1 M] HCl: Computational studies (DFT, MC and MD simulations), *Journal of Materials Research and Technology*, **9**, 2691 (2020). Doi: <https://doi.org/10.1016/j.jmrt.2020.01.002>
 25. R. Hsissou, O. Dagdag, S. About, F. Benhiba, M. Berardi, M. El Bouchti, A. Berisha, N. Hajjaji, A. Elharfi, Novel derivative epoxy resin TGETET as a corrosion inhibition of E24 carbon steel in 1.0 M HCl solution. Experimental and computational (DFT and MD simulations) methods, *Journal of Molecular Liquids*, **284**, 182 (2019). Doi: <https://doi.org/10.1016/j.molliq.2019.03.180>
 26. O. Dagdag, A. Berisha, Z. Safi, O. Hamed, S. Jodeh, C. Verma, E.E.E. Ebenso, A. El Harfi, DGEBA-polyaminoamide as effective anti-corrosive material for 15CDV6 steel in NaCl medium: Computational and experimental studies, *Journal of Applied Polymer Science*, **137**, 48402 (2020). Doi: <https://doi.org/10.1002/app.48402>
 27. O. Dagdag, R. Hsissou, A. El Harfi, A. Berisha, Z. Safi, C. Verma, E.E.E. Ebenso, M. Ebn Touhami, M. El Gouri, Fabrication of polymer based epoxy resin as effective anti-corrosive coating for steel: Computational modeling reinforced experimental studies, *Surfaces and Interfaces*, **18**, 100454 (2020). Doi: <https://doi.org/10.1016/j.surfin.2020.100454>
 28. H. Sun, Z. Jin, C. Yang, R.L.C. Akkermans, S .H. Robertson, N. A. Spentley, S. Miller, S. M. Todd, COMPASS II: extended coverage for polymer and drug-like mole-

- cule databases, *Journal of Molecular Modeling*, **22**, 1 (2016). Doi: <https://doi.org/10.1007/s00894-016-2909-0>
29. M. El Faydy, F. Benhiba, A. Berisha, Y. Kerroum, C. Jama, B. Lakhrissi, A. Guenbour, I. Warad, A. Zarrouk, An experimental-coupled empirical investigation on the corrosion inhibitory action of 7-alkyl-8-Hydroxyquinolines on C35E steel in HCl electrolyte, *Journal of Molecular Liquids*, **317**, 113973 (2020). Doi: <https://doi.org/10.1016/j.molliq.2020.113973>
 30. A. Berisha, Experimental, Monte Carlo and Molecular Dynamic Study on Corrosion Inhibition of Mild Steel by Pyridine Derivatives in Aqueous Perchloric Acid, *Electrochem*, **1**, 188 (2020). Doi: <https://doi.org/10.3390/electrochem1020013>
 31. O. Dagdag, R. Hsissou, A. Berisha, H. Erramli, O. Hamed, S. Jodeh, A. El Harfi, Polymeric-Based Epoxy Cured with a Polyaminoamide as an Anticorrosive Coating for Aluminum 2024-T3 Surface: Experimental Studies Supported by Computational Modeling, *Journal of Bio- and Tribo-Corrosion*, **5**, 58 (2019). Doi: <https://doi.org/10.1007/s40735-019-0251-7>
 32. O. Dagdag, R. Hsissou, A. El Harfi, Z. Safi, A. Berisha, C. Verma, E. E. Ebenso, M. A. Quraishi, N. Wazzan, S. Jodeh, M. El Gouri, Epoxy resins and their zinc composites as novel anti-corrosive materials for copper in 3% sodium chloride solution: Experimental and computational studies, *Journal of Molecular Liquids*, **315**, 113757 (2020). Doi: <https://doi.org/10.1016/j.molliq.2020.113757>
 33. S.J.H.M. Jessima, A. Berisha, S. S. Srikandan, S. Subhashini, Preparation, characterization, and evaluation of corrosion inhibition efficiency of sodium lauryl sulfate modified chitosan for mild steel in the acid pickling process, *Journal of Molecular Liquids*, **320**, 114382 (2020). Doi: <https://doi.org/10.1016/j.molliq.2020.114382>
 34. R. Hsissou, O. Dagdag, S. About, F. Benhiba, M. Berradi, M. El Bouchti, A. Berisha, N. Hajjaji, A. Elharfi, Novel derivative epoxy resin TGETET as a corrosion inhibition of E24 carbon steel in 1.0 M HCl solution. Experimental and computational (DFT and MD simulations) methods, *Journal of Molecular Liquids*, **284**, 182 (2019). Doi: <https://doi.org/10.1016/j.molliq.2019.03.180>
 35. R. Hsissou, B. Benzidia, M. Rehioui, M. Berradi, A. Berisha, M. Assouag, N. Hajjaji, A. Elharfi, Anticorrosive property of hexafunctional epoxy polymer HGTMDE for E24 carbon steel corrosion in 1.0 M HCl: gravimetric, electrochemical, surface morphology and molecular dynamic simulations, *Polymer Bulletin*, **77**, 3577 (2020). Doi: <https://doi.org/10.1007/s00289-019-02934-5>
 36. S. El Arrouji, K. Karrouchi, A. Berisha, K. Ismaily Alaoui, I. Warad, Z. Rais, S. Radi, M. Taleb, M. Ansar, A. Zarrouk, New pyrazole derivatives as effective corrosion inhibitors on steel-electrolyte interface in 1 M HCl: Electrochemical, surface morphological (SEM) and computational analysis, *Colloids and Surfaces A Physicochemical and Engineering Aspects*, **604**, 125325 (2020). Doi: <https://doi.org/10.1016/j.colsurfa.2020.125325>
 37. S. About, M. Zouarhi, D. Chebabe, M. Damej, A. Berisha, N. Hajjaji, Galactomannan as a new bio-sourced corrosion inhibitor for iron in acidic media, *Heliyon*, **6**, e03574 (2020). Doi: <https://doi.org/10.1016/j.heliyon.2020.e03574>
 38. M. Rbaa, P. Dohare, A. Berisha, O. Dagdag, L. Lakhrissi, M. Galai, B. Lakhrissi, M.E. Touhami, I. Warad, A. Zarrouk, New Epoxy sugar based glucose derivatives as eco friendly corrosion inhibitors for the carbon steel in 1.0 M HCl: Experimental and theoretical investigations, *Journal of Alloys and Compounds*, **833**, 154949 (2020). Doi: <https://doi.org/10.1016/j.jallcom.2020.154949>
 39. R. Hsissou, S. About, A. Berisha, M. Berradi, M. Assouag, N. Hajjaji, A. Elharfi, Experimental, DFT and molecular dynamics simulation on the inhibition performance of the DGDCBA epoxy polymer against the corrosion of the E24 carbon steel in 1.0 M HCl solution, *Journal of Molecular Structure*, **1182**, 340 (2019). Doi: <https://doi.org/10.1016/j.molstruc.2018.12.030>
 40. S.J.H.M. Jessima, A. Berisha, S. S. Srikandan, S. Subhashini, Preparation, characterization, and evaluation of corrosion inhibition efficiency of sodium lauryl sulfate modified chitosan for mild steel in the acid pickling process, *Journal of Molecular Liquids*, **320**, 114382 (2020). Doi: <https://doi.org/10.1016/j.molliq.2020.114382>
 41. O. Dagdag, A. Berisha, Z. Safi, S. Dagdag, M. Berrani, S. Jodeh, C. Verma, E.E.E.E. Ebenso, N. Wazzan, A. El Harfi, Highly durable macromolecular epoxy resin as anticorrosive coating material for carbon steel in 3% NaCl: Computational supported experimental studies, *Journal of Applied Polymer Science*, **137**, 49003 (2020). Doi: <https://doi.org/10.1002/app.49003>
 42. R. Hsissou, S. About, A. Berisha, M. Berradi, M. Assouag, N. Hajjaji, A. Elharfi, Experimental, DFT and molecular dynamics simulation on the inhibition performance of the DGDCBA epoxy polymer against the corrosion of the E24 carbon steel in 1.0 M HCl solution, *Journal of Molecular Structure*, **1182**, 340 (2019). Doi: <https://doi.org/10.1016/j.molstruc.2018.12.030>

43. A. Berisha, Ab initio exploration of nanocarbons as potential corrosion inhibitors, *Computational and Theoretical Chemistry*, **1201**, 113258 (2021). Doi: <https://doi.org/10.1016/j.comptc.2021.113258>
44. P.K.P.K. Uppalapati, A. Berisha, K. Velmurugan, R. Nandhakumar, A. Khosla, T. Liang, Salen type additives as corrosion mitigator for Ni–W alloys: Detailed electronic/atomic scale computational illustration, *International Journal of Quantum Chemistry*, **121**, e26600 (2020). Doi: <https://doi.org/10.1002/qua.26600>
45. S.J.H.M. Jessima, S. Subhashini, A. Berisha, A. Oral, S. S. Srikandan, Corrosion mitigation performance of disodium EDTA functionalized chitosan biomacromolecule - Experimental and theoretical approach, *International Journal of Biological Macromolecules*, **178**, 477 (2021). Doi: <https://doi.org/10.1016/j.ijbiomac.2021.02.166>
46. R. Hsissou, S. Abbout, A. Berisha, M. Berradi, M. Assouag, N. Hajjaji, A. Elharfi, Experimental, DFT and molecular dynamics simulation on the inhibition performance of the DGDCBA epoxy polymer against the corrosion of the E24 carbon steel in 1.0 M HCl solution, *Journal of Molecular Structure*, **1182**, 340 (2019). Doi: <https://doi.org/10.1016/j.molstruc.2018.12.030>
47. O. Dagdag, A. El Harfi, L. El Gana, Z. S. Safi, L. Guo, A. Berisha, C. Verma, E. E. Ebenso, N. Wazzan, M. El Gouri, Designing of phosphorous based highly functional dendrimeric macromolecular resin as an effective coating material for carbon steel in NaCl: Computational and experimental studies, *Journal of Applied Polymer Science*, **138**, 49673 (2021). Doi: <https://doi.org/10.1002/app.49673>
48. R. Oukhrib, Y. Abdellaoui, A. Berisha, H. Abou Oualid, J. Halili, K. Jusufi, M. Ait El Had, H. Bourzi, S. El Issami, F. A. Asmary, V. S. Parmar, C. Len, DFT, Monte Carlo and molecular dynamics simulations for the prediction of corrosion inhibition efficiency of novel pyrazolynucleosides on Cu(111) surface in acidic media, *Scientific Reports*, **11**, 3771 (2021). Doi: <https://doi.org/10.1038/s41598-021-82927-5>
49. R. Hsissou, B. Benzidia, M. Rehioui, M. Berradi, A. Berisha, M. Assouag, N. Hajjaji, A. Elharfi, Anticorrosive property of hexafunctional epoxy polymer HGTMDAE for E24 carbon steel corrosion in 1.0 M HCl: gravimetric, electrochemical, surface morphology and molecular dynamic simulations, *Polymer Bulletin*, **77**, 3577 (2020). Doi: <https://doi.org/10.1007/s00289-019-02934-5>